Chapter 4
Nanomaterials for Advanced Analytical Applications in Chemo- and Biosensors

Selvaraj Devi and Vairaperumal Tharmaraj

Contents

Abstract Nanomaterials with unique optical properties and biocompatibility have been widely employed for designing and fabricating highly selective and sensitive nanosensors for the detection of various chemical and biological species. The development of nanomaterial-based chemo- and biosensors is studied usually under direct spectroscopic and reagent-mediated sensor platforms using both unmodified and surface-functionalized nanomaterials. This chapter mainly focuses on selective sensing of chemical and biological molecules using various types of nanomaterials. The main readouts are absorption (colorimetric, UV-visible), fluorescence, Raman/SERS spectroscopic, and electrochemical sensing techniques. The detailed discussion on the design of nanomaterial-based sensing systems, sensing

S. Devi
Department of Inorganic Chemistry, University of Madras, Guindy, Chennai, India

V. Tharmaraj (✉)
Department of Analytical Chemistry, National Chung-Hsing University, Taichung, Taiwan

Mu. Naushad et al. (eds.), *Advanced Nanostructured Materials for Environmental Remediation*, Environmental Chemistry for a Sustainable World 25,
https://doi.org/10.1007/978-3-030-04477-0_4

principle, sensing method, and their signaling mechanisms has been provided. The sensing systems can also be ideally utilized for real-time applications.

Keywords Nanomaterials · Chemosensors · Biosensors · Absorption · Fluorescence · SERS and electrochemical sensors

4.1 Introduction

The recognition and sensing of chemical and biologically important species have emerged as significant goals in the field of nanosensors in recent years (Quang and Kim 2010; Zhou et al. 2011; Kim et al. 2011). Nanostructured materials are of great interest due to their size- and shape-dependent physical and chemical properties (Ferrando et al. 2008; Huynh et al. 2002; Kumar et al. 2016). There is also an increased interest in the synthesis of more complex nanostructures such as core-shell and hollow particles for advanced applications in chemical and biological sensing (Liang et al. 2009; Taton et al. 2000). The design and fabrication of nanomaterial-based sensors have generated great interest in detection of chemical and biological important target species with high precision and accuracy (Awual et al. 2015; Borisov and Wolfbeis 2008; Jung et al. 2010). The detection of the targeted species typically occurs through a controlled binding event and is then transmitted as a readable signal. A variety of signaling procedures are used for nanoparticle-based sensor with light absorption or either through fluorescence (Descalzo et al. 2005; Doleman et al. 2007) or scattering or current and potential changes (Zhan and Bard 2007).

Several analytical techniques, such as resonance Rayleigh scattering (Wen et al. 2013; Zhan et al. 2012), atomic absorption spectrometry (AAS) (Gao et al. 2012), inductively coupled plasma mass spectrometry (ICP-MS) (Chen et al. 2010), cold vapor atomic fluorescence spectrometry (Zhang et al. 2010), attenuated total reflectance Fourier-transform infrared spectroscopy (ATR-FTIR) (Vigano et al. 2005), etc., have been developed for sensing chemical and biological molecules. Most of the analytical techniques are more expensive and time-consuming processes. Consequently, high selectivity and sensitivity with simple instruments and easy operation have received much attention in recent years. Absorption spectroscopy (colorimetric/UV-visible), fluorescence spectroscopy, Raman spectroscopy, and electrochemistry are powerful analytical techniques for qualitative and quantitative sensing of chemical and biological molecules, as they offer simple handling, easy interpretation, moderate cost, portability, and fast analysis of the samples.

In general, sensors involve interaction between the target molecule (analyte) and a receptor (chemical or biological) that is signaled by an easily detectable change (Fabbrizzi and Poggi 1995). Most sensors depend on the binding mechanism or a chemical reaction to change the reporter characteristics (De Silva et al. 1997). All the

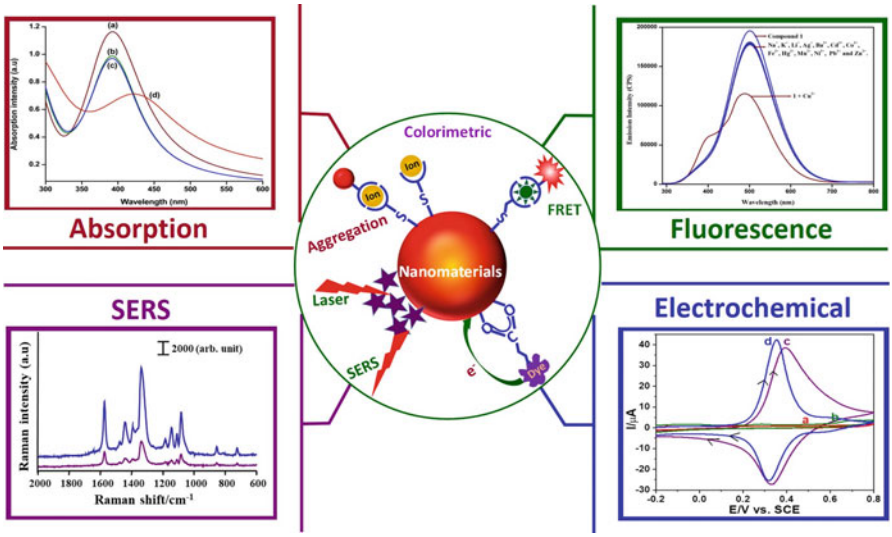

Fig. 4.1 Schematic illustration of signal amplification strategies using unmodified and surface-functionalized nanomaterials for sensing via absorption, fluorescence, SERS and electrochemical methods

sensors have been synthesized along these strategies for the detection of chemical and biological important analytes. According to the current IUPAC's definition "A chemical or bio-sensor is a device that transforms chemical information, ranging from the concentration of a specific sample component to total composition analysis, into an analytically useful signal." Optical reporter absorption (colorimetric and UV-visible), fluorescence, Raman spectroscopy, and electrochemical sensing have been widely used in this context (De Silva et al. 2009; Nguyen and Anslyn 2006), owing to a usually fast and convenient implementation. The instrumentation required for the use of such techniques is relatively simple and cheap which makes the quite attraction of sensors. However, the development of sensors is not trivial; materials science, molecular recognition, and device implementation are some of the aspects that play a significant role in the design of sensors.

In order to obtain the excellent selectivity and high sensitivity of chemical and biosensing, specific recognition and/or signal triggering elements are introduced which should be functionalized on the surface of nanomaterials with appropriate methods. The various approaches (Fig. 4.1) for the functionalization of nanoparticles (NPs) usually include noncovalent interaction such as physical adsorption, specific affinity interaction, and entrapment of chemical or biomolecules around the nanoparticles and covalent interaction of chemical or biomolecules with the functional groups on the nanoparticle surface (Veiseh et al. 2010). In signal amplification strategies, the nanomaterials usually act as catalysts to trigger the detectable signal or carriers for high loading of signal tags.

4.2 Principle and Operation Stages of a Sensor (Fig. 4.2)

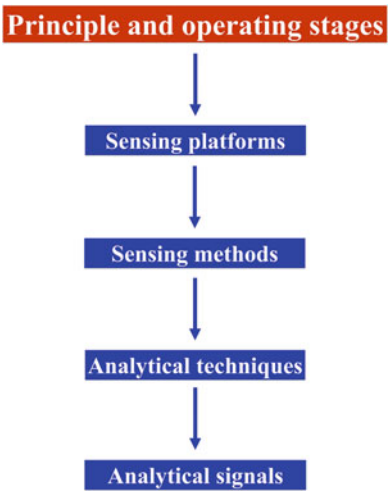

Fig. 4.2 Sensors principle and operation stages of a sensing system

4.3 Structure Adopted for Nanomaterial-Based Chemo- and Biosensors

The development of nanomaterial-based chemical and biological sensors is typically under direct spectroscopic and reagent-mediated sensors using both unmodified and surface-functionalized nanomaterials. This chapter exclusively deals with powerful analytical techniques such as absorption spectroscopy (colorimetric/UV-visible), fluorescence spectroscopy, Raman spectroscopy, and electrochemistry. The detection of analyte is directly based on some fundamental optical or electrical property via color changes/absorption, emission, scattering, or current and/or potential changes. The whole structure of this chapter is shown in Fig. 4.3.

4.4 Nanomaterials as Sensing Platforms

The development of nanomaterial-based sensors is usually achieved either in unmodified or in functionalized nanoparticles.

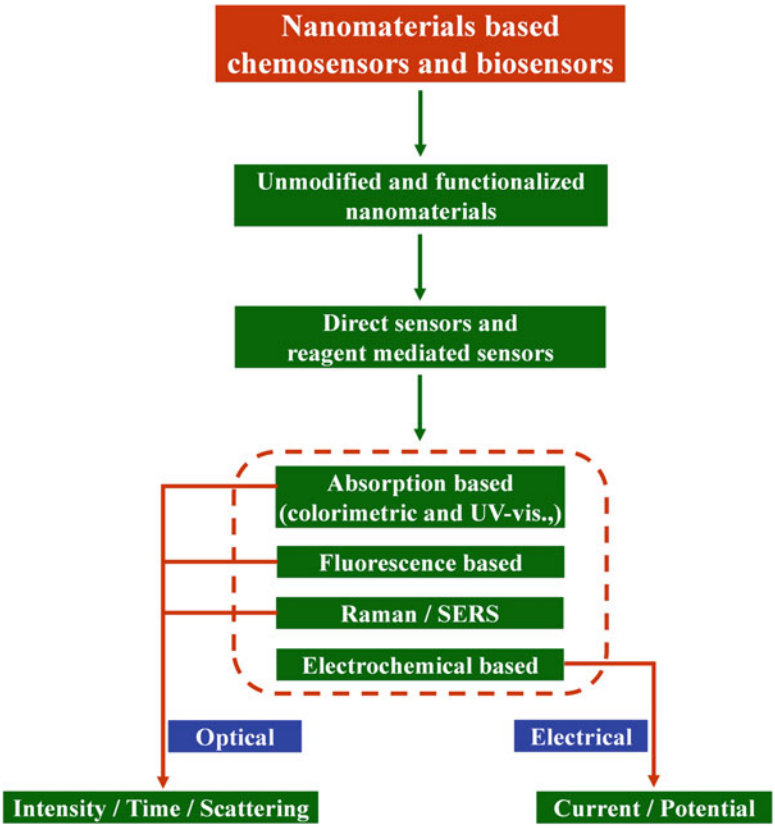

Fig. 4.3 Sensing platform for nanomaterial-based chemo- and biosensors

4.4.1 Unmodified Nanoparticles

Unmodified metallic nanoparticle surface has positive charge with flexible high affinity toward negatively charged ones. This affinity differences offer many advantages; since different sizes and shapes of metallic nanoparticle solution have different stability, they give various color signals.

4.4.2 Functionalized Nanoparticles

Nanoparticles can be converted into powerful nanoscale chemo- and biosensors by functionalizing their surface with specific binding receptors and/or reporter molecules such as nucleic acids, proteins, dyes, and fluorescent tags. In addition, many

other specific organic compounds which introduce new functionality will enhance their selectivity and sensitivity of target molecules.

4.5 Sensing Methods

In general, chemo- and biosensors may be categorized under two types: (i) direct sensors and (ii) reagent-mediated sensors.

4.5.1 Direct Spectroscopy Sensing

In a direct sensor, the analyte is detected directly via the basic phenomenon; localized surface plasmon resonance (LSPR) is responsible for the brilliant colors exhibited by the metal nanoparticles under illumination. Various direct sensor techniques are widely used, but this chapter exclusively deals with UV-visible and fluorescence spectroscopic methods and Raman/surface-enhanced Raman spectroscopy (SERS) measurements.

4.5.2 Reagent-Mediated Sensing

In a reagent-mediated sensing system, the change in analytical response is coming from the intermediate reagent. For example, analyte concentration is monitored from the analyte sensitive dye molecule or catalyst. This chapter mainly deals about only two types of reagent-mediated sensors, namely, colorimetric sensing and electrochemical sensors.

4.6 Analytical Techniques and Signals

4.6.1 UV-Visible Absorption-Based Sensors

UV-visible absorption spectroscopy is an important analytical technique for sensor application, as it offers simple handling, easy interpretation, moderate cost, portability, and fast analysis of the samples. To design nanomaterial-based sensing platform for the detection of environmental pollution materials (heavy and biological essential metal ions) and biomolecules, researchers have utilized the nanoparticle aggregation- or disaggregation-induced color change that reflects a redshift in the extinction spectrum (Polavarapu et al. 2014; Zhai et al. 2014). Based on this principle, simple and rapid colorimetric detection of Cu^{2+} ions in aqueous medium

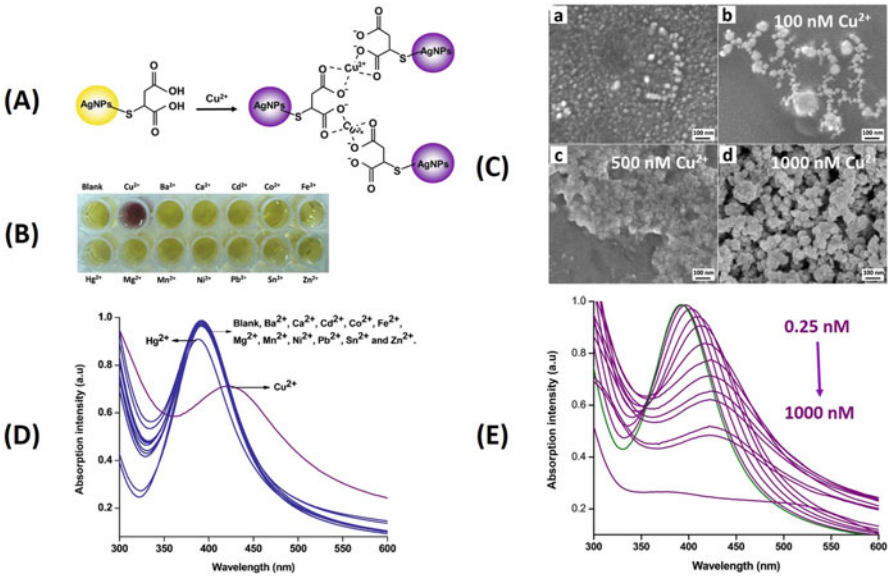

Fig. 4.4 (**A**) Schematic diagram for the interaction of TMA-AgNPs with Cu^{2+}. (**B**) Photograph of TMA-AgNPs (0.25 mM) in presence of Cu^{2+} and various metal ions (500 nM). (**C**) SEM images of TMA-AgNPs (a), TMA-AgNPs in the presence of 100 nM (b), 500 nM (c), and 1000 nM (d) of Cu^{2+} ions. (**D**) UV-visible spectra of TMA-AgNPs (0.25 mM) in the presence of Cu^{2+} and various other metal ions (100 nM) in aqueous medium. (**E**) UV-visible spectra of TMA-AgNPs (0.25 mM) upon addition of Cu^{2+} from 0.25 to 1000 nM in aqueous medium

via aggregation of thiomalic acid-functionalized Ag nanoparticles (TMA-AgNPs) has been developed as shown in Fig. 4.4A (Tharmaraj and Jyisy 2014). A visually detectable color change from yellow to purple in the presence of Cu^{2+} ion over other metal ions was observed (Fig. 4.4B). The aggregation behavior was confirmed by SEM images of TMA-AgNPs and TMA-AgNPs in the presence of 100 nM, 500 nM, and 1000 nM Cu^{2+} which is shown in Fig. 4.4C. TMA-AgNPs can be aggregated only in the presence of Cu^{2+} that cause a redshift of SPR band from 392 to 423 nm as observed in UV-visible spectra (Fig. 4.4D). Sensitivity response of TMA-AgNPs to Cu^{2+} was estimated in the concentration ranges of Cu^{2+} from 0.25 nM to 1000 nM, and their corresponding UV-visible spectra are shown in Fig. 4.4E. This chemosensor has excellent selectivity and sensitivity for Cu^{2+}, and the detection limit is as low as 0.25 nM and also successfully applied for the detection of copper ion in real water samples.

A simple, selective, and sensitive colorimetric detection of Hg^{2+} was achieved in aqueous medium using soaproot plant-stabilized silver nanoparticles by biologically green synthesis (Farhadi et al. 2012). In the presence of Hg^{2+}, the yellow AgNP solution was turned to colorless, accompanying the broadening and blueshifting of SPR band. This sensing method has been applied for real sample analysis, and the detection limit is as low as 2.2 μM. The selective detection of Co^{2+} ion on different

Table 4.1 List of UV-visible absorption-based colorimetric sensors

Nanomaterial probes	Analyte	Mechanisms	Limit of detection	Linear range	References
Tripolyphosphate-modified AgNPs	Mn^{2+}	Aggregation	0.1 μM	0.05–20 μM	Gao et al. (2013)
Ascorbic acid-capped AgNPs	Cr_6^{2+}	Aggregation	0.5 nM	0.07–1.84 μM	Wu et al. (2013)
Dendrimer-stabilized AgNPs	Hg^{2+}	Aggregation	10 ppb	10 ppb–10 ppm	Yuan et al. (2013)
Starch-stabilized AgNPs	Cu^{2+}	Aggregation	0.5 μM	0.1–10 μM	Miao et al. (2013)
Unmodified AuNPs	Cysteine	Aggregation	0.01 ppm	0.1–0.6 ppm	Jongjinakool et al. (2014)
Valine-capped AgNPs	Pb^{2+}	Aggregation	30.5 μM	0–100 ppm	Priyadarshini and Pradhan (2017)
Peptide-capped AuNP	Ni^{2+}	Aggregation	34 nM	60–160 nM	Parnsubsakula et al. (2018)
Mercaptosuccinic acid-modified AuNPs	Cr^{3+}	Aggregation	0.04 μM	0.6–1.4 μM	Yu et al. (2017)
Ligand-stabilized AuNPs	Pd^{2+}	Aggregation	4.23 μM	1–100 μM	Anwar et al. (2018)
Functionalized AgNPs	Ni^{2+}	Aggregation	0.6 μM	4.0–60 μM	Feng et al. (2017)

shapes of (nanosphere, nanoplate, and nanorod) glutathione-modified silver nanoparticles (GSH-AgNPs) is based on aggregation by the formation of chelating complex between Co^{2+} ion and COO^{-} groups of glutathione (Sung et al. 2013). Selective colorimetric detection for Cu^{2+}- and lidocaine hydrochloride (LC-HCl)-based sensor was developed by the aggregation of homocysteine-functionalized silver nanoparticles (Dou et al. 2013) that result in the color change from deep brown to bright yellow, and the SPR intensity characterized at 571 nm was found to be proportional to the concentration of Cu^{2+} ions, and the detection limit is as low as 3.2 nM. "Mix-and-detect" rapid virtual colorimetric ultrasensitive detection of Hg^{2+} ion using label-free cysteamine-capped AgNPs has been developed (Bhattacharjee and Chakraborty 2014). In the presence of Hg^{2+} ion, thiophillic Hg^{2+} would lead to partial exchange of cysteamine ligand with the detection limit of 275 pM. Some recent reports for UV-visible absorption method-based sensing systems are listed in Table 4.1.

4.6.2 Fluorescence-Based Sensors

Fluorescence spectroscopy is one of the most powerful ultrasensitive analytical techniques when compared to other analytical methods which make the detection

of single molecules. Also this approach provides a limit of detection (LOD = 3.3σ/S, where σ is standard deviation of the response and S is the slope of the calibration curve) at a signal-to-noise (S/N) ratio for the detection up to parts-per-trillion level with good precision and accuracy (Wang et al. 2014; Nolan and Lippard 2008). Design of nanomaterial-based fluorescent sensors for quick detection of targets molecules has been developed either by fluorescent enhancement (turn on) or quenching (turn off) that controls the response through both energy and electron transfer processes (Liu et al. 2014; Jia et al. 2014).

Alginate-stabilized silver nanocubes (AgNCbs) bound to rhodamine 6G (Rh6G) composite as selective sensor for Hg^{2+} ion in aqueous solution have been developed (Tharmaraj and Pitchumani 2011) with the detection limit as low as 0.1 nM. Rh6G dye molecules bound to AgNCbs surface were observed in quenching the fluorescence; when there is presence of Hg^{2+} ion, bound Rh6G is released from the alginate-AgNCb surfaces which indicate a large fluorescence restoration with a concomitant color change from yellow to purple. Ratiometric fluorescence probe is designed and developed (Niu et al. 2015) by linking with two parts, positively charged aggregation-induced emission (AIE) organic fluorescence nanoparticles (OFNPs) as the reference and negatively charged Au nanoclusters (Au NCs) as the response. This probe can be used to detect Hg^{2+} and also melamine, since red fluorescence of Au NCs can be quenched by mercury ions and recovered by melamine, due to the strong affinity between metallophilic Hg^{2+}–Au and Hg^{2+}–N. This dual-emission ratiometric fluorescence probe has good biocompatibility; hence it is applicable for biological imaging and detection.

Thiol-DNA-functionalized gold nanoparticles (AuNPs) as a simple fluorescence spectrometric sensor for Hg^{2+} detection in aqueous solution were developed (Wang et al. 2015). Hg^{2+} is selectively induced conformational change of single-stranded DNA (ssDNA) with an enhanced fluorescence resonance energy transfer (FRET) process between the energy donor (fluorescein, FAM) and the energy acceptor (AuNPs). The assay enables the detection limit as low as 8 nM and also applied to monitor Hg^{2+} in tap water samples. Noncross-linking aggregation of fluorosurfactant-capped silver nanoparticles for colorimetric sensing of cysteine was developed (Chen et al. 2014). High specificity toward cysteine was observed as the nonionic fluorosurfactant ligand thiol-silver interaction prohibited the binding of other functional groups on the surface of AgNPs. This sensing probe can be successfully applied for the determination of cysteine in human urine and plasma samples with the detection limit as low as 0.05 μM.

Dansyl fluorophore-functionalized thiol-stabilized AgNPs containing 2-aminothiophenol units with excellent selective binding sites for Cu^{2+} ion were developed, and energy transfer (ET) from the dansyl moiety to the copper complex occurs that causes the fluorescent ratiometric response as seen in Fig. 4.5A (Tharmaraj and Pitchumani 2013). High-resolution transmission electron microscopy (HRTEM) images of highly dispersed thiol-stabilized silver nanoparticles, 2D lattice fringe spacing image, and selected area electron diffraction (SAED) pattern are shown in Fig. 4.5B(a-d). The particle size and lattice fringes of AgNP were 5.5 nm and 0.2 nm, respectively. The lattice planes of nano silver were observed in

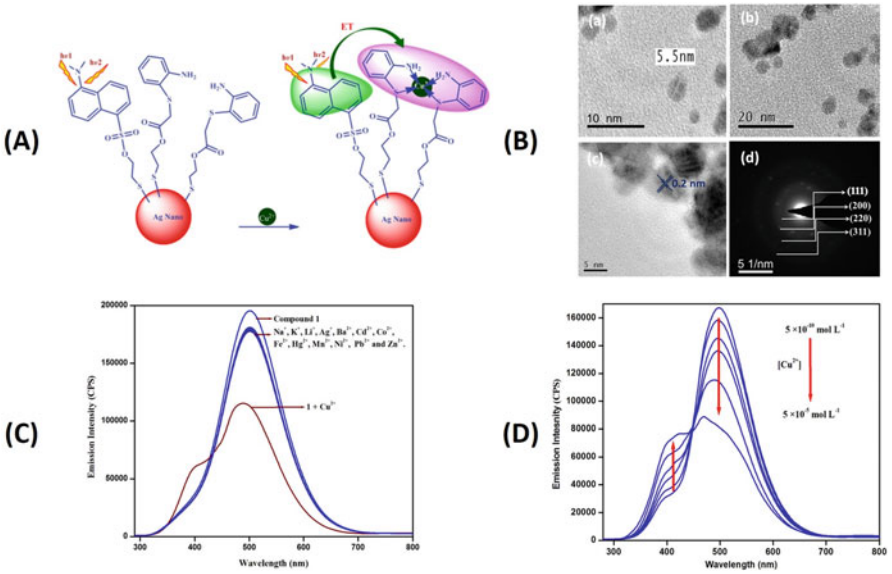

Fig. 4.5 (**A**) Schematic diagram proposed binding mechanisms for dansyl-AgNPs with Cu^{2+} ion. (**B**) (a), (b) HRTEM images of highly dispersed thiol-stabilized AgNPs. (c) The 2D lattice fringes of HRTEM image. (d) Selected area diffraction pattern is showing the corresponding planes. (**C**) Fluorescence spectra of dansyl-AgNPs (1 mg mL^{-1}) in the presence of Cu^{2+} and various other metal ions (0.5 μM). (**D**) Fluorescence spectra of dansyl-AgNPs (1 mg mL^{-1}) upon addition of Cu^{2+} from 0.5 nM to 0.5 μM

SAED pattern. Selectivity of fluorescent ratiometric response for the decrease in fluorescence at 497 nm and an increase in fluorescence at 410 nm with an isoemissive point at 445 nm was favored only in the presence of Cu^{2+} ions, whereas other metal ions led to no fluorescence ratiometric change as seen in Fig. 4.5C. Sensitivity response of dansyl-AgNPs to Cu^{2+} was evaluated in the concentration ranges of Cu^{2+} from 0.5 nM to 0.5 μM, and their corresponding fluorescence spectra is shown in Fig. 4.5D.

Some recent reports for fluorescence method-based sensing systems are listed in Table 4.2.

4.6.3 Raman/Surface-Enhanced Raman Spectroscopy (SERS) Sensors

Raman spectroscopy is one of the important analytical techniques used in the field of sensors for identification of specific molecules. But traditional Raman spectroscopy has very poor efficiency of inelastic scattering processes with relatively weak signal. In recent years these problems are overcome by developing advanced method like

Table 4.2 List of fluorescence sensors based on nanomaterials

Nanomaterial probes	Sensing strategy	Analyte	Mechanisms	Limit of detection	References
3-Mercaptopropionic acid-capped CdS quantum dots	Turn off-on	Lysozyme	Displacement	6.3 nM	Liu et al. (2016)
AuNPs and porous silicon nanoparticles	Turn off-on	L-Cysteine	FRET	35 μM	Zhang and Jia (2017)
Gold nanoparticles	Electrostatic interaction	Melamine	FRET	0.18 μg L^{-1}	Cao et al. (2014)
Carbon dots	Quenching effect	Hydroquinone (H_2Q)	Electron transfer	0.1 μM	Ni et al. (2015)
BODIPY-functionalized AuNPs	Turn on	Cysteine	Displacement	1.2 μM	Lo et al. (2015)

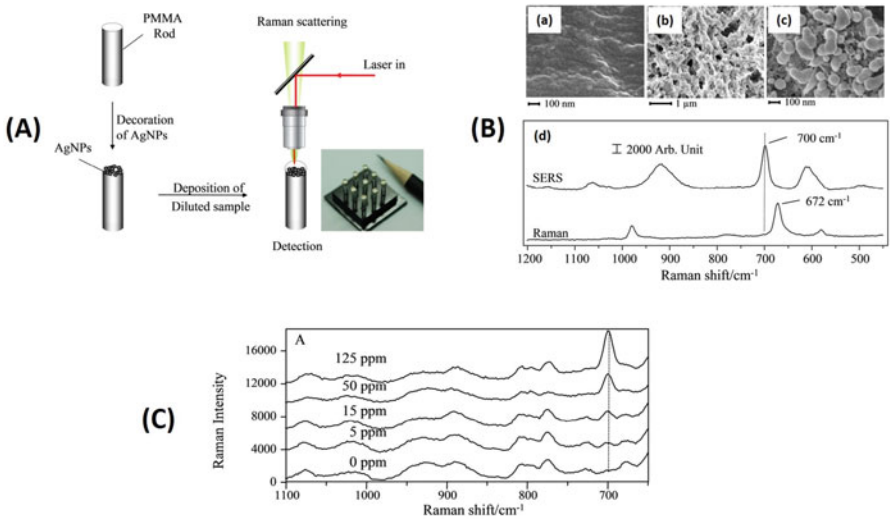

Fig. 4.6 (**A**) Schematic diagram of SERS detection of target molecules using droplet-based method. (**B**) SEM images of bare PMMA rod (a), PVDF-coated rod (b), and AgNPs decorated on PVDF-coated rod (c). Raman spectra of solid melamine and SERS spectra of melamine in water (400 ppb) detected by cylindrical substrate (d). (**C**) SERS spectra of melamine in milk liquid at 0, 5, 15, 50 and 125 ppm

surface-enhanced Raman spectroscopy (SERS). In SERS, the target molecule is brought into close proximity to a metallic (typically Ag, Au, or Cu) surface with nanoscopically defined features or in solution next to a nanoparticle with a diameter much smaller than the wavelength of the excitation light.

Silver nanoparticle decorated on filter paper as a highly sensitive surface-enhanced Raman scattering (SERS) substrate was fabricated for detection of tyrosine in aqueous solution (Cheng et al. 2011) with the detection limit as low as 625 nM. The Raman labels to use for detection of protein and protein concentration assay were developed (Han et al. 2010) which uses the SERS signal of Coomassie Brilliant Blue dye adsorbed nonspecifically to silver colloids for monitoring the total protein concentration.

Silver nanoparticles decorated on a cylindrical support was developed (Rajapandiyan et al. 2011) for the detection of melamine in milk liquid and powder samples by surface-enhanced Raman spectroscopy (SERS) technique. Figure 4.6A illustrates the detection procedures in the cylindrical SERS substrate. Cylindrical SERS substrate was prepared by decoration of silver nanoparticles (AgNPs) on a solid support of polymethyl methacrylate (PMMA) rod by silver mirror reaction. SEM images show the PMMA surface roughness was increased after treating with PVDF solution. Also, the size of the formed AgNPs was around 200 nm in diameter with the Raman spectra of solid melamine and SERS spectra of melamine as shown in Fig. 4.6B. Sensitivity response of AgNP cylindrical substrate to the melamine

Table 4.3 List of SERS sensors based on nanomaterials

Nanomaterials probes	Analyte	Limit of detection	References
Silver nanoparticles	Rhodamine 6G	Single molecule	Nie and Emery (1997)
Au electrode	Adenine	0.01 pM	Cho et al. (2009)
Au-SiO_2 core-shell NPs	Nile blue A, toluidine blue O, and methylene blue	NA	Fernandez-Lopez et al. (2009)
Ag-Au core-shell NPs	Adenosine triphosphate, hemoglobin, and myoglobin	NA	Kumar et al. (2007)
Star-shaped AuNPs	1-Naphthalenethiol, Alexa Fluor 750, and phenol	NA	Rodriguez-Lorenzo et al. (2010)
AgNPs	Yeast cells W303-1A	Subcellular level	Sujith et al. (2009)
Au-Ag core-shell NPs on Fe_3O_4 hybrid nanospheres	4-Aminothiophenol	NA	Guo et al. (2009a, b)
TiO_2 NPs	4-Mercaptobenzoic acid	0.1 μM	Yang et al. (2009)
AuNPs	2,4,6-TNT	$<1 \times 10^{-10}$ g	
Au-Ag core-shell NPs on multiwalled carbon nanotube	Adenine and 4-aminothiophenol	NA	Guo et al. (2009a, b)

concentration ranges was tested up to 125 ppm, and their corresponding SERS spectra are shown in Fig. 4.6C.

Some recent reports for SERS method-based sensing systems are listed in Table 4.3.

4.6.4 Electrochemical-Based Sensors

Electrochemical methods have been used extremely in analysis of biological and environmental interest compounds due to their advantages such as quick response, wide linear dynamic range, simplicity, reliability, reproducibility, inherent miniaturization, low cost, low-power requirements, and high selectivity and sensitivity. The type of electrical signal used for quantitation distinguishes the various electroanalytical techniques. For example, in case of voltammetry, the current is measured as a function of changing potential that can be applied in different ways (linear, cyclic, anodic stripping voltammetry). Amperometric measurements are performed by maintaining a constant potential at the working electrode with respect to reference electrode and measuring the generated current. The generated potentials or currents are related to the contents of analyte in the test solution (Zoski 2007). The researchers first tried to detect compounds using carbon and metal electrodes without

any chemical modification. But the problems such as oxidation or reduction occur at high over potential, suffer from interferences and kinetically sluggish. Therefore, the development of electrochemical sensor based on chemically modified electrodes for estimating biologically important compounds is a rapidly growing area of electrochemistry to overcome the problems associated with bare electrodes. Particularly, the chemically modified electrodes have been fabricated using nanomaterials such as metal nanoparticles, metal oxide nanomaterials, and carbon nanomaterials.

Silver nanoparticles incorporated within the mesoporous silicate framework of zeolite Y-modified glassy carbon electrode-based electrochemical sensor were developed for the simultaneous detection of dopamine (DA) and uric acid (UA) (Meenakshi et al. 2016). The oxidation of DA and UA was obtained at +0.31 V and +0.43 V (vs. Ag/AgCl) using AgNPs/Zeo-Y/GCE under the optimum experimental condition. A well-resolved peak potential window (~120 mV) for the oxidation of both DA and UA was observed at AgNPs/Zeo-Y/GCE system. This is due to the strong electrostatic interaction between the positively charged DA and negatively charged silver nanoparticles embedded in zeolite Y which facilitates the electron transfer process is favorable and the oxidation peak potential of DA is resolved against UA. The detection limits of DA and UA were found to be 1.6×10^{-8} M and 2.51×10^{-8} M in the linear range of 0.02×10^{-6} to 0.18×10^{-6} M ($R^2 = 0.9899$) and 0.05×10^{-6} to 0.7×10^{-6} M ($R^2 = 0.9996$) by using differential pulse voltammetry (DPV) method.

The electrochemical oxidation of paracetamol (PAR) and caffeine (CAF) using nickel hexacyanoferrate-decorated titanium nanotube (TNT)-modified glassy carbon electrode was developed (Fig. 4.7A) (Devi and Pandian 2014). The SEM image of TNT shows the formation of tube-like structure with the external diameter of 10–80 nm ranges and several micrometers in length. The TEM image shows that the TNT wall consists of two layers with an average external diameter of 28 nm. After surface modification with NiHCF, the size and shape of TNT become expanded with the uniform deposition of NiHCF on both inner and outer surfaces (Fig. 4.7B). DPV experiment was carried out for the simultaneous detection of PAR and CAF with well-separated peak potentials. The determination of PAR has been done separately in the concentration ranges of 1.3–10.7 μM with the solution containing 6 μM CAF (Fig. 4.7C). Similarly, the determination of CAF has been studied in the concentration ranges of 7.3–18.7 μM in presence of PAR at a fixed concentration of 1.3 μM (Fig. 4.7D). The detection limits of PAR and CAF are found to be 29.5 and 18.2 nM, respectively. Some recent reports for electrochemical method-based sensing systems are listed in Table 4.4.

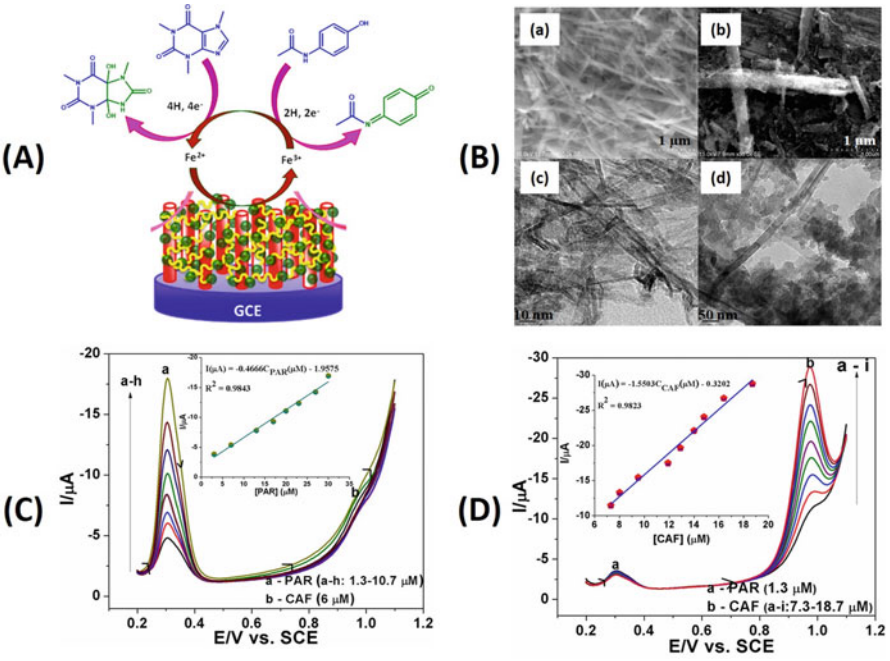

Fig. 4.7 (**A**) Mechanisms for the oxidation of paracetamol and caffeine at NiHCF/TNT@GCE. (**B**) FE-SEM and HR-TEM images of TNT (a and c) and NiHCF/TNT (b and d). (**C**) DPV of CS-NiHCF@TNT/GCE at concentration of PAR (a–h, 1.3–10.7 μM) and 6 μM of CAF. (**D**) DPV of CS-NiHCF@TNT/GCE at concentration of CAF (a–i, 7.3–18.7 μM) and 1.3 μM of PAR. The inset shows the calibration plot

Table 4.4 List of electrochemical sensors based on nanomaterials

Nanomaterial probes	Analyte	Method	Limit of detection	References
CS@PPY/CS_2	Hg^{2+}	DPV	1.8 μM	Devi et al. (2014)
DNA-SWCNT	Pb^{2+}	DPV	0.4 nM	Lian et al. (2014)
AgNPs-GO	As^{3+}	SW-ASV	0.24 nM	Dar et al. (2014)
Aptamer-AuNPs	Cu^{2+}	SWV	0.1 pM	Noroozifar et al. (2011)
NiHCF@TiO_2/GCE	Nitrites	DPV	0.11 μM	Sophia et al. (2012)
Ag nanostructure/gold electrode	Ascorbic acid	DPV	0.01 mM	Zheng et al. (2013)
Au/Pt/Pd/TiO_2 NTs	Dopamine	DPV	0.03 μM	Mahshid et al. (2011)
Manganese vanadate nanorods/GCE	Cysteine	CV	0.026 μM	Pei et al. (2013)

4.7 Conclusions

Remarkable progress in the development of simple and efficient methods for sensing of chemical and biomolecules utilizing nanomaterials has been made over the past several years. The successful development of sensors with high selectivity and sensitivity for specific, toxic, heavy/biologically essential metal ions and biomolecules to detect in real-time monitoring was clearly demonstrated. In this chapter, we believed that most promising results and remarkable sensing system in terms of high selectivity and sensitivity have been discussed. However, many of the absorption- and fluorescence-based sensing systems were operated in aqueous medium, and some other system using nonaqueous solvents was applied for real sample analysis. Fluorescence sensors based on surface-functionalized nanomaterials have been widely used in biological and environmental sample analysis, due to their high sensitivity, low cost, and commercial availability. SERS technique has great promise for chemical and biosensing applications based on design of paper, and also fiber-based SERS active substrates have very high surface area with flexibility for efficient analysis of biological live samples. Electrochemical techniques are coupled with nanomaterials that have been used for the development of electrochemical sensors. The attractive design and fabrication of nanomaterial-based electrochemical sensing systems can offer a highly selective increase in sensitivity and reproducibility. Most of the sensing systems with a very low detection limits (in the range of ppb) were thus achieved and applied for the real sample analysis.

References

Anwar A, Minhaz A, Khan NA, Kalantari K, Afifi ABM, Shah MR (2018) Synthesis of gold nanoparticles stabilized by a pyrazinium thioacetate ligand: a new colorimetric nanosensor for detection of heavy metal Pd(II). Sensors Actuators B 257:875–881. https://doi.org/10.1016/j.snb.2017.11.040

Awual MR, Hasan MM, Naushad M et al (2015) Preparation of new class composite adsorbent for enhanced palladium(II) detection and recovery. Sensors Actuators B Chem 209:790–797. https://doi.org/10.1016/j.snb.2014.12.053

Bhattacharjee Y, Chakraborty A (2014) Label-free cysteamine-capped silver nanoparticle-based colorimetric assay for hg(ii) detection in water with subnanomolar exactitude. ACS Sustain Chem Eng 2:2149–2154. https://doi.org/10.1021/sc500339n

Borisov SM, Wolfbeis OS (2008) Optical biosensors. Chem Rev 108(2):423–461. https://doi.org/10.1021/cr068105t

Cao X, Shen F, Zhang M, Guo J, Luo Y, Xu J, Li Y, Sun C (2014) Highly sensitive detection of melamine based on fluorescence resonance energy transfer between rhodamine B and gold nanoparticles. Dyes Pigments 111:9–107. https://doi.org/10.1016/j.dyepig.2014.06.001

Chen B, Heng S, Peng H, Hu B, Yu X, Zhang Z, Pang D, Yue X, Zhu Y (2010) Magnetic solid phase microextraction on a microchip combined with electrothermal vaporization-inductively coupled plasma mass spectrometry for determination of Cd, Hg and Pb in cells. Anal At Spectrom 25:1931–1938. https://doi.org/10.1039/C0JA00003E

Chen S, Gao H, Shen W, Lu C, Yuan Q (2014) Colorimetric detection of cysteine using noncrosslinking aggregation of fluorosurfactant-capped silver nanoparticles. Sens Actuators B Chem 190:673–678. https://doi.org/10.1016/j.snb.2013.09.036

Cheng ML, Tsai BC, Yang J (2011) Silver nanoparticle-treated filter paper as a highly sensitive surface-enhanced Raman scattering (SERS) substrate for detection of tyrosine in aqueous solution. Anal Chim Acta 708(1–2):89–96. https://doi.org/10.1016/j.aca.2011.10.013

Cho HS, Lee B, Liu GL, Agarwal A, Lee LP (2009) Label-free and highly sensitive biomolecular detection using SERS and electrokinetic preconcentration. Lab Chip 9:3360–3363. https://doi.org/10.1039/B912076A

Dar RA, Khare NG, Cole DP, Karna SP, Srivastava AK (2014) Green synthesis of a silver nanoparticle–graphene oxide composite and its application for As(III) detection. RSC Adv 4:14432–14440. https://doi.org/10.1039/C4RA00934G

De Silva AP, Gunaratne HQN, Gunnlaugsson T, Huxley AJM, McCoy CP, Rademacher JT, Rice TE (1997) Signaling recognition events with fluorescent sensors and switches. Chem Rev 97 (5):1515–1566. https://doi.org/10.1021/cr960386p

De Silva AP, Moody TS, Wright GD (2009) Fluorescent PET (photoinduced electron transfer) sensors as potent analytical tools. Analyst 134(12):2385–2393. https://doi.org/10.1039/b912527m

Descalzo AB, Rurack K, Weisshoff H, Martınez-Manez R, Marcos MD, Amoros P, Hoffmann K, Soto J (2005) Rational design of a chromo- and fluorogenic hybrid chemosensor material for the detection of long-chain carboxylates. J Am Chem Soc 127(1):184–200. https://doi.org/10.1021/ja045683n

Devi S, Pandian K (2014) Synthesis of chitosan protected nickel hexacyanoferrate modified titanium oxide nanotube and study its application on simultaneous s electrochemical detection of paracetamol and caffeine. Adv Mater Res 938(2014):192–198. https://doi.org/10.4028/www.scientific.net/AMR.938.192

Devi S, Devasena T, Saratha S, Tharmaraj P, Pandian K (2014) Dithiocarbamate post functionalized polypyrrole modified carbon sphere for the selective and sensitive detection of mercury by voltammetry method. Int J Electrochem Sci 9:670–683

Doleman L, Davies L, Rowe L, Moschou EA, Deo S, Daunert S (2007) Bioluminescence DNA hybridization assay for Plasmodium falciparum based on the photoprotein aequorin. Anal Chem 79(11):4149–4153. https://doi.org/10.1021/ac0702847

Dou Y, Yang X, Liu Z, Zhu S (2013) Homocysteine-functionalized silver nanoparticles for selective sensing of Cu^{2+} ions and lidocaine hydrochloride. Colloids Surf A Physicochem Eng Asp 423:20–26. https://doi.org/10.1016/j.colsurfa.2013.01.027

Fabbrizzi L, Poggi A (1995) Sensors and switches from supramolecular chemistry. Chem Soc Rev 24:197–202. https://doi.org/10.1039/CS9952400197

Farhadi K, Forougha M, Molaei R, Hajizadeha S, Rafipour A (2012) Highly selective Hg^{2+} colorimetric sensor using green synthesized and unmodified silver nanoparticles. Sensors Actuators B Chem 161:880–885. https://doi.org/10.1016/j.snb.2011.11.052

Feng J, Jin W, Huang P, Wu F (2017) Highly selective colorimetric detection of Ni^{2+} using silver nanoparticles cofunctionalized with adenosine monophosphate and sodium dodecyl sulfonate. J Nanopart Res 19:306. https://doi.org/10.1007/s11051-017-3998-0

Fernandez-Lopez C, Mateo-Mateo C, Alvarez-Puebla RA, Perez-Juste J, Pastoriza-Santos I, Liz-Marzan LM (2009) Highly controlled silica coating of PEG-capped metal nanoparticles and preparation of SERS-encoded particles. Langmuir 25(24):13894–13899. https://doi.org/10.1021/la9016454

Ferrando R, Jellinek J, Johnston RL (2008) Nanoalloys: from theory to applications of alloy clusters and nanoparticles. Chem Rev 108(3):845–910. https://doi.org/10.1021/cr040090g

Gao Y, Shi Z, Long Z, Wu P, Zheng C, Hou X (2012) Determination and speciation of mercury in environmental and biological samples by analytical atomic spectrometry. Microchem J 103:1–14. https://doi.org/10.1016/j.microc.2012.02.001

Gao YX, Xin JW, Shen ZY, Pan W, Li X, Wu AG (2013) A new rapid colorimetric detection method of Mn^{2+} based on tripolyphosphate modified silver nanoparticles. Sensors Actuators B 181:288–293. https://doi.org/10.1016/j.snb.2013.01.079

Guo S, Dong S, Wang E (2009a) A general route to construct diverse multifunctional Fe_3O_4/metal hybrid nanostructures. Chem Eur J 15(10):2416–2424. https://doi.org/10.1002/chem.200801942

Guo SJ, Li J, Ren W, Wen D, Dong SJ, Wang EK (2009b) Carbon nanotube/silica coaxial nanocable as a three-dimensional support for loading diverse ultra-high-density metal nanostructures: facile preparation and use as enhanced materials for electrochemical devices and SERS. Chem Mater 21(11):2247–2257. https://doi.org/10.1021/cm900300v

Han XX, Xie Y, Zhao B, Ozaki Y (2010) Highly sensitive protein concentration assay over a wide range via surface-enhanced Raman scattering of Coomassie brilliant blue. Anal Chem 82 (11):4325–4328. https://doi.org/10.1021/ac100596u

Huynh WU, Dittmer JJ, Alivisatos AP (2002) Hybrid nanorod-polymer solar cells. Science 295 (5564):2425–2427. https://doi.org/10.1126/science.1069156

Jia J, Wu A, Luan S (2014) Synthesis and investigation of the imprinting efficiency of ion imprinted nanoparticles for recognizing copper. Phys Chem Chem Phys 16:16158–16165. https://doi.org/10.1039/C4CP01858C

Jongjinakool S, Palasak K, Bousod N, Teepoo S (2014) Gold nanoparticles-based colorimetric sensor for cysteine detection. Energy Procedia 56:10–18. https://doi.org/10.1016/j.egypro.2014.07.126

Jung JH, Park M, Shinkai S (2010) Fabrication of silica nanotubes by using self-assembled gels and their applications in environmental and biological fields. Chem Soc Rev 39:4286–4302. https://doi.org/10.1039/C002959A

Kim HN, Guo Z, Zhu W, Yoon J, Tian H (2011) Recent progress on polymer-based fluorescent and colorimetric chemosensors. Chem Soc Rev 40:79–93. https://doi.org/10.1039/C0CS00058B

Kumar GVP, Shruthi S, Vibha B, Reddy BAA, Kundu TK, Narayana C (2007) Hot spots in Ag Core−Au shell nanoparticles potent for surface-enhanced Raman scattering studies of biomolecules. J Phys Chem C 111(11):4388–4392. https://doi.org/10.1021/jp068253n

Kumar A, Guo C, Sharma G et al (2016) Magnetically recoverable ZrO2/Fe3O4/chitosan nanomaterials for enhanced sunlight driven photoreduction of carcinogenic Cr(VI) and dechlorination & mineralization of 4-chlorophenol from simulated waste water. RSC Adv 6:13251–13263. https://doi.org/10.1039/C5RA23372K

Lian Y, Yuan M, Zhao H (2014) DNA wrapped metallic single-walled carbon nanotube sensor for Pb (II) detection. Fullerenes, Nanotubes, Carbon Nanostruct 22(5):510–518. https://doi.org/10.1080/1536383X.2012.690462

Liang CH, Wang CC, Lin YC, Chen CH, Wong CH, Wu CY (2009) Iron oxide/gold core/shell nanoparticles for ultrasensitive detection of carbohydrate−protein interactions. Anal Chem 81 (18):7750–7756. https://doi.org/10.1021/ac9012286

Liu J, Zuo W, Zhang W, Liu J, Wang Z, Yang Z, Wang B (2014) Europium(III) complex-functionalized magnetic nanoparticle as a chemosensor for ultrasensitive detection and removal of copper(II) from aqueous solution. Nanoscale 6:11473–11478. https://doi.org/10.1039/C4NR03454F

Liu X, Na W, Qua Z, Su X (2016) Turn-off–on fluorescence probe based on 3-mercaptopropionic acid-capped CdS quantum dots for selective and sensitive lysozyme detection. RSC Adv 6:85795–85801. https://doi.org/10.1039/C6RA14420A

Lo SH, Wu MC, Wu SP (2015) A turn-on fluorescent sensor for cysteine based on BODIPY functionalized Au nanoparticles and its application in living cell imaging. Sensors Actuators B Chem 221:1366–1371. https://doi.org/10.1016/j.snb.2015.08.015

Mahshid S, Li C, Mahshid SS, Askari M, Dolati A, Yang L, Luo S, Cai Q (2011) Sensitive determination of dopamine in the presence of uric acid and ascorbic acid using TiO_2 nanotubes modified with Pd, Pt and Au nanoparticles. Analyst 136(11):2322–2329. https://doi.org/10.1039/c1an15021a

Meenakshi S, Devi S, Pandian K, Devendiran R, Selvaraj M (2016) Sunlight assisted synthesis of silver nanoparticles in zeolite matrix and study of its application on electrochemical detection of dopamine and uric acid in urine samples. Mater Sci Eng C 69:85–94. https://doi.org/10.1016/j.msec.2016.06.037

Miao LJ, Xin JW, Shen ZY, Zhang YJ, Wang HY, Wu AG (2013) Exploring a new rapid colorimetric detection method of Cu^{2+} with high sensitivity and selectivity. Sensors Actuators B 176:906–912. https://doi.org/10.1016/j.snb.2012.10.070

Nguyen BT, Anslyn EV (2006) Indicator-displacement assays. Coord Chem Rev 250 (23–24):3118–3127. https://doi.org/10.1016/j.ccr.2006.04.009

Ni P, Dai H, Li Z, Sun Y, Hu J, Jiang S, Wang Y, Li Z (2015) Carbon dots based fluorescent sensor for sensitive determination of hydroquinone. Talanta 144:258–262. https://doi.org/10.1016/j.talanta.2015.06.014

Nie SM, Emery SR (1997) Probing single molecules and single nanoparticles by surface-enhanced Raman scattering. Science 275(5303):1102–1106

Niu C, Liu Q, Shang Z, Zhaoa L, Ouyang J (2015) Dual-emission fluorescent sensor based on AIE organic nanoparticles and Au nanoclusters for the detection of mercury and melamine. Nanoscale 7:8457–8465. https://doi.org/10.1039/C5NR00554J

Nolan EM, Lippard SJ (2008) Tools and tactics for the optical detection of mercuric ion. Chem Rev 108(9):3443–3480. https://doi.org/10.1021/cr068000q

Noroozifar M, Khorasani-Motlagh M, Taheri A (2011) Determination of cyanide in wastewaters using modified glassy carbon electrode with immobilized silver hexacyanoferrate nanoparticles on multiwall carbon nanotube. J Hazard Mater 185(1):255–261. https://doi.org/10.1016/j.jhazmat.2010.09.02

Parnsubsakula A, Oaewb S, Surareungchai W (2018) Zwitterionic peptide-capped gold nanoparticles for colorimetric detection of Ni^{2+}. Nanoscale 10:5466–5473. https://doi.org/10.1039/C7NR07998B

Pei LZ, Pei YQ, Xie YK, Fan CG, Yu HY (2013) Synthesis and characterization of manganese vanadate nanorods as glassy carbon electrode modified materials for the determination of L-cysteine. Cryst Eng Comm 15:1729–1738. https://doi.org/10.1039/C2CE26592C

Polavarapu L, Perez-Juste J, Xu QH, Liz-Marzan LM (2014) Optical sensing of biological, chemical and ionic species through aggregation of plasmonic nanoparticles. J Mater Chem C 2:7460–7476. https://doi.org/10.1039/C4TC01142B

Priyadarshini E, Pradhan N (2017) Metal-induced aggregation of valine capped gold nanoparticles: an efficient and rapid approach for colorimetric detection of Pb^{2+} ions. Sci Rep 7:9278. https://doi.org/10.1038/s41598-017-08847-5

Quang DT, Kim SJ (2010) Fluoro- and chromogenic chemodosimeters for heavy metal ion detection in solution and biospecimens. Chem Rev 110(10):6280–6301. https://doi.org/10.1021/cr100154p

Rajapandiyan P, Tang WL, Yang J (2011) Rapid detection of melamine in milk liquid and powder by surface-enhanced Raman scattering substrate array. Food Control 56:155–160. https://doi.org/10.1016/j.foodcont.2015.03.028

Rodriguez-Lorenzo L, Alvarez-Puebla RA, de Abajo FJG, Liz-Marzan LM (2010) Surface enhanced Raman scattering using star-shaped gold colloidal nanoparticles. J Phys Chem C 114(16):7336–7340. https://doi.org/10.1021/jp909253w

Sophia SJ, Devi S, Pandian K (2012) Electrocatalytic oxidation of hydrazine based on NiHCF@TiO_2 core- shell nanoparticles modified GCE. Int J Electrochem Sci 7:6580–6598

Sujith A, Itoh T, Abe H, Yoshida KI, Kiran MS, Biju V, Ishikawa M (2009) Imaging the cell wall of living single yeast cells using surface-enhanced Raman spectroscopy. Anal Bioanal Chem 394 (7):1803–1809. https://doi.org/10.1007/s00216-009-2883-9

Sung HK, Oh SY, Park C, Kim Y (2013) Colorimetric detection of Co^{2+} ion using silver nanoparticles with spherical, plate, and rod shapes. Langmuir 29:8978–8982. https://doi.org/10.1021/la401408f

Taton TA, Mirkin CA, Letsinger RL (2000) Scanometric DNA array detection with nanoparticle probes. Science 289(5485):1757–1760

Tharmaraj V, Jyisy Y (2014) Sensitive and selective colorimetric detection of Cu^{2+} in aqueous medium via aggregation of thiomalic acid functionalized Ag nanoparticles. Analyst 139:6304–6309. https://doi.org/10.1039/c4an01449a

Tharmaraj V, Pitchumani K (2011) Alginate stabilized silver nanocube–Rh6G composite as a highly selective mercury sensor in aqueous solution. Nanoscale 3:1166–1170. https://doi.org/10.1039/C0NR00749H

Tharmaraj V, Pitchumani K (2013) A highly selective ratiometric fluorescent chemosensor for Cu (II) based on dansyl-functionalized thiol stabilized silver nanoparticles. J Mater Chem B 1:1962–1967. https://doi.org/10.1039/C3TB00534H

Veiseh O, Gunn JW, Zhang MQ (2010) Design and fabrication of magnetic nanoparticles for targeted drug delivery and imaging. Adv Drug Deliv Rev 62(3):284–304. https://doi.org/10.1016/j.addr.2009.11.002

Vigano C, Ruysschaert JM, Goormaghtigh E (2005) Sensor applications of attenuated total reflection infrared spectroscopy. Talanta 65(5):1132–1142. https://doi.org/10.1016/j.talanta.2004.07.052

Wang F, Wang L, Chen X, Yoon J (2014) Recent progress in the development of fluorometric and colorimetric chemosensors for detection of cyanide ions. Chem Soc Rev 43:4312–4324. https://doi.org/10.1039/C4CS00008K

Wang G, Lu Y, Yan C, Lu Y (2015) DNA-functionalization gold nanoparticles based fluorescence sensor for sensitive detection of Hg^{2+} in aqueous solution. Sensors Actuators B Chem 211:1–6. https://doi.org/10.1016/j.snb.2015.01.051

Wen G, Lin C, Tang M, Liu G, Liang A, Jiang Z (2013) A highly sensitive aptamer method for Ag+ sensing using resonance Rayleigh scattering as the detection technique and a modified nanogold probe. RSC Adv 3:1941–1946. https://doi.org/10.1039/C2RA22542E

Wu X, Xu Y, Dong Y, Jiang X, Zhu N (2013) Colorimetric determination of hexavalent chromium with ascorbic acid capped silver nanoparticles. Anal Methods 5:560. https://doi.org/10.1039/c2ay25989c

Yang LB, Jiang X, Ruan WD, Zhao B, Xu WQ, Lombardi JR (2009) Adsorption study of 4-MBA on TiO2 nanoparticles by surface-enhanced Raman spectroscopy. J Raman Spectrosc 40:2004–2008. https://doi.org/10.1002/jrs.2358

Yu Y, Hong Y, Wang Y, Sun X, Liu B (2017) Mercaptosuccinic acid modified gold nanoparticles as colorimetric sensor for fast detection and simultaneous identification of Cr^{3+}. Sensors Actuators B 239:865–873. https://doi.org/10.1016/j.snb.2016.08.043

Yuan X, Wen S, Shena M, Shi X (2013) Dendrimer-stabilized silver nanoparticles enable efficient colorimetric sensing of mercury ions in aqueous solution. Anal Methods 5:5486. https://doi.org/10.1039/c3ay41331d

Zhai D, Xu W, Zhang L, Chang YT (2014) The role of "disaggregation" in optical probe development. Chem Soc Rev 43:2402–2411. https://doi.org/10.1039/C3CS60368G

Zhan W, Bard AJ (2007) Electrogenerated chemiluminescence. Immunoassay of human C-reactive protein by using $Ru(bpy)_3^{2+}$-encapsulated liposomes as labels. Anal Chem 79(2):459–463. https://doi.org/10.1021/ac061336f

Zhan S, Wu Y, He L, Wang F, Zhan X, Zhou P, Qiu S (2012) Measuring the size and density of nanoparticles by centrifugal sedimentation and flotation. Anal Methods 4:3997–4002. https://doi.org/10.1039/C8AY00237A

Zhang H, Jia Z (2017) Development of fluorescent FRET probes for "off-on" detection of L-cysteine based on gold nanoparticles and porous silicon nanoparticles in ethanol solution. Sensors 17(3):520. https://doi.org/10.3390/s17030520

Zhang WB, Su ZF, Chu XF, Yang XA (2010) Evaluation of a new electrolytic cold vapour generation system for mercury determination by AFS. Talanta 80(5):2106–2112. https://doi.org/10.1016/j.talanta.2009.11.016

Zheng Y, Huang Z, Zhao C, Weng S, Zheng W, Lin X (2013) A gold electrode with a flower-like gold nanostructure for simultaneous determination of dopamine and ascorbic acid. Microchim Acta 180(7–8):537–544. https://doi.org/10.1007/s00604-013-0964-0

Zhou Y, Xu Z, Yoon J (2011) Fluorescent and colorimetric chemosensors for detection of nucleotides, FAD and NADH: highlighted research during 2004–2010. Chem Soc Rev 40:2222–2235. https://doi.org/10.1039/C0CS00169D

Zoski CG (2007) Handbook of electrochemistry. Elsevier, Oxford